



Tropical Journal of Natural Product Research

Available online at <https://www.tjnpr.org>

Original Research Article



Potential of *Ganoderma applanatum* Extract as Anticancer and Immunomodulator in Diethylnitrosamine-induced Colon Cancer

Siti Rahayu¹, Aulia Umi Rohmatika^{2,3}, Ufairanisa Islamatasya², Mochammad Aqilah Herdiansyah², Raden Joko Kuncoroningrat Susilo⁴, Suhailah Hayaza⁴, Djoko Santoso⁵, Odi Yoshitaka Anggarda⁶, Sri Puji Astuti Wahyuningsih⁷, Win Darmanto^{7,8*}

¹Doctoral Program in Biology, Faculty of Science and Technology, Universitas Airlangga, Surabaya, 60115, Indonesia

²Magister Program in Biology, Faculty of Science and Technology, Universitas Airlangga, Surabaya, 60115, Indonesia

³Faculty of Medicine, Universitas Pembangunan Nasional "Veteran", Surabaya, 60293, Indonesia

⁴Nanotechnology Engineering, Faculty of Advance Technology and Multidiscipline, Universitas Airlangga, Surabaya, 60115, Indonesia

⁵Faculty of Medicine, Universitas Airlangga, Surabaya, 60115, Indonesia

⁶RSUD. Sayang, Cianjur, 43216, Indonesia

⁷Department of Biology, Faculty of Science and Technology, Universitas Airlangga, Surabaya, 60115, Indonesia

⁸Institute of Science, Technology, and Health, Jombang 61419, Indonesia

ARTICLE INFO

Article history:

Received 11 March 2025

Revised 29 July 2025

Accepted 02 August 2025

Published online 01 October 2025

ABSTRACT

Ganoderma applanatum extract (GAE) exhibits numerous biological activities, particularly anticancer and immunomodulatory activities. This study aimed to examine the effect of GAE on colonic goblet cells, Lieberkuhn crypts, CD4+ and CD8+ cells in mice spleen. Mice were randomly divided into four groups (n = 6): normal control (KN) group given only distilled water, negative control (K-) group administered 100 mg/kg BW diethylnitrosamine (DEN), positive control (K+) group administered 100 mg/kg BW DEN + 10 mg/kg BW doxorubicin, and extract treatment (P) group administered 100 mg/kg BW DEN + 150 mg/kg BW GAE. Colon histology was assessed using haematoxylin and eosin staining. CD4+ and CD8+ percentages were determined by flow cytometry. Molecular docking of selected bioactive compounds of GAE with CD4+ (PDB ID: 1CDJ) and CD8+ (PDB ID: 1CD8) was performed using PyMol v1.74 and PyRx 0.8 software, with visualization using BIOVIA Discovery Studio 2019 and molecular dynamics via CABS-flex webserver. GAE significantly increased the number of goblet cells and Lieberkuhn crypt height in mice colon, with values of 28.00 ± 4.05 and 29.24 ± 4.61 μ m, respectively. GAE improved colon histology and enhanced immunomodulation by increasing CD4+ and CD8+ cells in mice spleen, with values of $21.98 \pm 3.03\%$, and $8.34 \pm 0.86\%$, respectively. Molecular docking indicated lucidenic B had the highest binding affinity against CD4+ cells, while β -glucan had the highest binding affinity against CD8+ cells. Molecular dynamics confirmed complex stability (Root mean square fluctuation (RMSF) < 3 Å), suggesting stable ligand-receptor interactions in the plasma.

Keywords: *Ganoderma applanatum*, Colon Cancer, Immunomodulator, Histology, Molecular Docking.

Copyright: © 2025 Rahayu *et al.* This is an open-access article distributed under the terms of the [Creative Commons Attribution License](https://creativecommons.org/licenses/by/4.0/), which permits unrestricted use, distribution, and reproduction in any medium, provided the original author and source are credited.

Introduction

According to Global Cancer Observatory (Globocan) data 2020, colorectal cancer is the third most common cancer after breast and lung cancer. Several factors contribute to an increased susceptibility to colorectal cancer, including the presence of polyps, genetic predisposition, abnormal genes, intestinal inflammation, smoking, habitual consumption of alcohol, frequent intake of red and processed meats, obesity, diabetes mellitus, and infections caused by bacteria such as *Helicobacter pylori* and *Fusobacterium* spp. Colorectal cancer develops when the gene responsible for coding tumor suppressor proteins in colon cells undergoes mutation. This mutation results in the

dysfunction and activation of the proto-oncogene (K-Ras gene), converting it into an oncogene. When the K-Ras gene is mutated, cells lose the ability to break down GTP into GDP, leading to uncontrolled cell division and growth, eventually forming cancer that can metastasize.¹ Diethylnitrosamine (DEN), a hazardous agent, can trigger cancer by increasing free radicals, which cause oxidative stress that transforms normal cells into cancer cells. Oxidative stress leads to inflammation in the colon, involving both local and systemic responses, contributing to tumor growth and organ dysfunction. Histologically, colon inflammation damages the epithelial cells of the mucosal layer, reduces the amount of goblet cells, and shortens the Lieberkuhn crypts. This inflammation also affects the lamina propria, further promoting the development of colon cancer.²

The pharmaceutical sector is rapidly advancing in the development of synthetic drugs for the treatment of cancer. However, these drugs sometimes have negative effects on the body. Cancer treatment techniques such as surgery, chemotherapy, and radiotherapy also come with adverse effects, making them less effective and often quite expensive. One type of antibiotic, doxorubicin, is widely recognized as the most effective anti-tumor agent for eliminating malignant cells and inducing tumor regression in various human neoplasms. However, its therapeutic applications are limited by adverse effects, which include immunosuppression, hepatotoxicity, nephrotoxicity, and cardiotoxicity.^{3,4}

*Corresponding author. E mail: windarmanto@fst.unair.ac.id

Tel: +

Citation: Rahayu S, Rohmatika AU, Islamatasya U, Herdiansyah MA, Susilo RJK, Hayaza S, Santoso D, Anggarda OY, Wahyuningsih SPA, Darmanto W. Potential of *Ganoderma applanatum* Extract as Anticancer and Immunomodulator in Diethylnitrosamine-induced Colon Cancer. Trop J Nat Prod Res. 2025; 9(9): 4310 – 4320 <https://doi.org/10.26538/tjnpr/v9i9.29>

Official Journal of Natural Product Research Group, Faculty of Pharmacy, University of Benin, Benin City, Nigeria

Cancer treatment is currently being optimized with the use of biological agents to mitigate the progression and malignancy associated with it.⁵ *Ganoderma applanatum* is a type of mushroom that exhibits antitumor and immunomodulatory effects that can be harnessed for cancer therapy as well as antibody production.⁶ This mushroom can act as a prebiotic to help improve the quality of life by reducing the chances of developing obesity, cancer, allergic reactions, cardiovascular diseases, and certain degenerative diseases.⁷ *G. applanatum* extract contains β -glucan, which is different from the polysaccharides present in other carbohydrate foods. This compound plays a crucial role in the medical field, particularly in immune system regulation. The β -glucan content in *Ganoderma* mushrooms has been shown to modulate the immune system and has the potential to exert tumor-inhibitory effects.⁸ These mushrooms offer various health benefits, including non-specific stimulation of the immune system, as well as hypocholesterolemic, hypoglycemic, anti-inflammatory, anticancer, and prebiotic effects.⁹ The development of *in silico* study of natural products is also widely carried out to predict the effect of medicinal compounds on body receptors. *In silico* is a predictive tool used to determine the binding affinity of ligands to receptors, and ligand-receptor complex interactions.¹⁰ Therefore, an *in silico* study of *Ganoderma* compounds on the immune receptors can be designed. Such types of immune receptors are the CD4+ (PDB ID: 1CDJ) and CD8+ (PDB ID: 1CD8) receptors. Both receptors modulate the body's immune system. An increase in the proportion of CD4+ and CD8+ cells will boost the immune system and improve immunity.

Despite the many studies that have explored the anticancer properties of GAE, its specific role in inhibiting colon cancer cells and modulating immune response remains unexplored. The current study addressed this gap by assessing the effects of *Ganoderma applanatum* extract on colonic histology - specifically goblet cell numbers and Lieberkuhn crypt height - as well as its immunomodulatory impact through changes in the percentage of splenic CD4+ and CD8+ cells. In addition, molecular docking and dynamics simulations were done in order to examine the interactions among the active compounds of *G. applanatum* and CD4+/CD8+ receptors to provide insight into their potential mechanism of action.

Materials and Methods

Collection and identification of fungal sample

Ganoderma applanatum fruiting body (basidiocarp). was collected from Pacet, Mojokerto, East Java, Indonesia (Latitude: -7.6679012° S, Longitude: 112.5385039° E). The fungus was identified at the Department of Biology, Faculty of Science and Technology, Universitas Airlangga, Surabaya, Indonesia, and assigned voucher number 29/09/JJ/2022.

Preparation of extract

The Mushrooms were cut into pieces, dried in the shade for 14 days, then ground into powder. *G. applanatum* powder (100 g) was boiled in water (2 L) at 60 – 65°C for 6 hours. The water extract was filtered and the residue was re-extracted following the same procedure. The combined filtrate was incubated at 25°C–30°C for 24 hours, and then freeze dried to give *G. applanatum* extract.

Anticancer and immunomodulatory activities screening

Animals

Twenty-four (24) female mice (*Mus musculus*) DDY strain aged 3 - 4 months and weighing between 30 - 40 g were obtained from Pusvetma Surabaya. The mice were kept in well-ventilated cages under standard laboratory condition. The mice were acclimatized to the laboratory condition for two weeks. They were fed with rodent pellets, and had free access to drinking water.

Ethical approval

This study was approved by the Animal Care and Use Committee, Faculty of Dentistry, Airlangga University, Indonesia, with approval reference number: 0570/HRECC.FODM/ VI/2024.

Experimental design

The mice were randomly allotted into four groups of six animals per group: Normal control (KN), Negative control (K-), Positive control

(K+), and *G. applanatum* extract treatment group (P). The normal control group (KN) were healthy mice, which were neither induced nor given any treatment. The negative control group (K-) was induced with Diethylnitrosamine (DEN) 100 mg/kg BW but did not receive any treatment. The positive control (K+) was induced with 100 mg/kg BW DEN and administered 10 mg/kg BW doxorubicin. The *G. applanatum* extract treatment group (P) was induced with 100 mg/kg BW DEN and administered 150 mg/kg BW *G. applanatum* extract. Doxorubicin and *G. applanatum* extract were administered by oral gavage once daily for one month.

A day after the last treatment, the mice were anesthetized using 2% xylazine (2 mg/kg BW) and 10% ketamine (15 mg/kg BW). The mice were dissected, and the colons were removed and cut about 3 cm above the rectum. The colons were placed in formalin solution for histological examination. The spleen were also collected and used for flow cytometric assay for CD4+ and CD8+.

Histological examination of the colon

Colon preparations were made using hematoxylin eosin staining (Sigma Aldrich, USA). First, the colon were fixed in neutral buffered formalin (Sigma Aldrich, USA) for 48 h, then cut lengthwise into two parts and placed in a tissue container (cassette). Tissue processing was accomplished manually by rehydrating the organs in a series of graded ethanol solutions (70%, 80%, and 96%), respectively, followed by clearing with xylol for 15 minutes in the first xylol solution and overnight in the second solution. Samples were subsequently embedded in paraffin blocks. The colon was cut into a 5 μ m thick tissue section with the aid of a rotary microtome. The tissue sections were stained with hematoxylin-eosin, and then examined for histological changes, such as amount of goblet cells and the height of Lieberkuhn crypts under a light microscope (OLYMPUS CX23, Japan) at 100X magnification.

Flow cytometry

In order to define the percentage of CD4+ and CD8+ T cells, FITC-conjugated anti-mouse CD4+ antibody and PE-conjugated anti-mouse CD8+ antibody (BioLegend, San Diego, USA) were used alongside a BD FACSVerser flow cytometer. Splenocytes were harvested at a concentration of 2×10^6 cells and placed into microcentrifugation tubes containing 500 μ L PBS (Sigma-Aldrich, USA). The cell suspensions were centrifuged at 2500 rpm for 5 minutes at a temperature of 10°C, after which the supernatant was discarded. The resulting pellets were incubated with 100 μ L of extracellular antibody solution (0.005 mg/100 μ L) at 4°C for 30 minutes in the dark. Subsequent to incubation, 200 μ L of fixative solution was added, and the samples were further incubated at 4°C for 20 minutes. The fixative was then eliminated by rinsing with 500 μ L of washperm solution, followed by centrifugation at 2500 rpm for 5 minutes at 10°C. Decanted supernatant was gently disposed, and the pellets were suspended in 100 μ L of intracellular antibody solution (0.005 mg/100 μ L) and incubated at 4°C for 20 minutes.

In silico study

Software

Molecular docking was performed on a Dell Vostro 14 3000 laptop with an AMD Ryzen 5 3500U processor. The system operates on Windows 10 Ultimate 64-bit and was equipped with Radeon Vega Mobile Gfx at 2.10 GHz.

Ligand preparation

Bioactive compounds identified in *G. applanatum* extract were obtained from the USDA phytochem webserver (<https://phytochem.nal.usda.gov/>). Further screening to optimize the drug-likeness of the identified compounds was carried out using the SCFBio webserver (<http://www.scfbio-iitd.res.in/software/drugdesign/LIP1.jsp>). Solubility of the compounds was analyzed through SwissADME webserver (<http://www.swissadme.ch>). Information related to canonical SMILES of compounds along with PDB ID was obtained from PubChem (<https://pubchem.ncbi.nlm.nih.gov/>).

Protein preparation

Protein (receptor) preparation was done by retrieving receptor files from Protein Data Banks (<https://www.rcsb.org/>). The receptors used were

CD4+ (PDB ID: 1CDJ) and CD8+ (PDB ID: 1CD8). Impurities such as water molecules and non-essential ligands were removed using PyMol v1.74 software (Schrödinger, LLC, USA). Molecular docking was conducted using PyRx 0.8 software (SourceForge Headquarters, San Diego, California, USA). Docking validation was performed using the CABS-flex webserver (<https://biocomp.chem.uw.edu.pl/CABSflex2/index>). Visualization of ligand-receptor complexes was assisted by BIOVIA Discovery Studio 2019 (Dassault Systemes BIOVIA, San Diego, California, USA).

Ligand selection

Thirty-four (34) ligands from *G. applanatum* were obtained from the USDA Phytochem webserver. The drug-likeness of the ligands were assessed based on the Lipinski's Rule of Five, and further screened using the SCFbio web server. The assessed parameters included molecular weight (g/mol), number of hydrogen bond acceptors and donors, logP (lipophilicity), and molar refractivity. Based on the screening results, all ligands showed potential as drug candidates. Subsequently, solubility screening was conducted using the SwissADME webserver. Of all the compounds, five compounds, including beta-glucan, ganoderic acid-M, lucidenic acid-B, lucidenic acid-C, and mannitol, which had the highest drug-likeness and solubility potential were selected. An increased solubility score suggests that the compound has a better capacity for leaching into the cellular environment. These selected ligands were then subjected to molecular docking experiments using CD4+ and CD8+ as test receptors.

Molecular docking

Molecular docking was conducted using PyRx 0.8 software (SourceForge Headquarters, San Diego, California, USA) to obtain the binding affinity between the ligand and its target receptor. The binding affinity denotes the energy generated in the ligand-protein complex. The more negative the value of the binding affinity, the higher the probability of triggering specific activity, such as inhibition.¹¹

Molecular docking validation

Validation of molecular docking was conducted using CABS-flex webserver (<https://biocomp.chem.uw.edu.pl/CABSflex2/index>).¹² The simulation entailed several parameters, notably protein rigidities, restraint settings, C-alpha restraints weight, side-chain restraint weight, trajectory, temperature range, number of cycles, and RNG seed.¹³ Receptor with the best binding affinity was used for the molecular docking validation.

Statistical analysis

Data were presented as mean \pm standard deviation (SD). Statistical analysis was performed using SPSS 21 software (SPSS Inc., Chicago, IL, USA). Data were subjected to One-Way analysis of variance (ANOVA), and differences between mean values were regarded as statistically significant at $p < 0.05$.

Results and Discussion

Effect of *G. applanatum* extract on goblet cells and Lieberkuhn crypts

Table 1 presents the number of goblet cells, height of Lieberkuhn crypts, and percentages of CD4+ and CD8+ cells in the various groups. There was significant disparities in these parameters among the groups, with the lowest levels found in the negative control group (K-). Figure 1 presents the photomicrograph of the histopathological sections of goblet cells and Lieberkuhn crypts across the different treatment groups. The photomicrograph indicates that administration of *G. applanatum* extract as a potential anticancer agent can help restore colon cells damaged by DEN exposure and slow the progression toward cancer. As indicated in Figure 2, the K- group showed the lowest number of goblet cells (19.17 ± 3.06), and this was significantly different from the other three groups: KN (28.50 ± 5.32), K+ (28.00 ± 2.61), and P (28.00 ± 4.50).

Table 1: Effect of *Ganoderma applanatum* extract on goblet cells, Lieberkuhn crypts, CD4+ cells and CD8+ cells

Indicator	Group			
	KN	K-	K+	P
Number of goblet cells	28.50 ± 5.32	19.17 ± 3.06	28.00 ± 2.61	28.00 ± 4.05
Height of Lieberkuhn crypts (μm)	31.22 ± 2.13	21.31 ± 2.56	26.03 ± 1.65	29.24 ± 4.61
Percentage of CD4+ cells (%)	19.32 ± 3.11	17.31 ± 2.80	21.84 ± 1.85	21.98 ± 3.03
Percentage of CD8+ cells (%)	7.41 ± 1.94	5.94 ± 0.99	8.03 ± 1.17	8.34 ± 0.86

KN: Normal control (given distilled water only); **K-:** Negative control (administered DEN at 100 mg/kg BW); **K+:** Positive control (administered DEN at 100 mg/kg BW + Doxorubicin at 10 mg/kg BW); **P:** (administered DEN at 100 mg/kg BW + *Ganoderma applanatum* extract at 150 mg/kg BW).

However, no significant differences were found among the KN, K+, and P treatment groups. Similarly, the K- group exhibited the lowest Lieberkuhn crypt height ($21.31 \pm 2.56 \mu\text{m}$), which was significantly different from that of the KN ($31.22 \pm 2.13 \mu\text{m}$), K+ ($26.03 \pm 1.65 \mu\text{m}$), and P group ($29.24 \pm 4.61 \mu\text{m}$) (Figure 3). No statistically significance difference was observed among the KN and P groups, nor between the K+ and P groups, suggesting a comparable effect of these treatments in promoting crypt regeneration.

Exposure to DEN increases methaemoglobin levels in the blood, leading to anaemia and tissue hypoxia.¹⁴ The resulting oxygen deficiency (hypoxia) causes cellular apoptosis. Reduced oxygen consumption in tissues decreases both the number and size of cell organelles and leads to cellular and tissue atrophy. Consequently, the reduced amount of goblet cells noticed in the K- group could be attributed to hypoxia-induced apoptosis.

Goblet cells are essential for preserving intestinal lining integrity by secreting mucus, providing a protective barrier against luminal aggressors.¹⁵ Under normal physiological conditions, goblet cells in the

colonic epithelium are uniformly distributed and exhibit a regular elliptical shape.¹⁶ Diethylnitrosamine (DEN), a nitrosamine compound, exhibits carcinogenic properties through the reaction between nitrites and secondary amines.¹⁷

Excessive accumulation of nitrosamines in the body stimulates the formation of reactive oxygen species (ROS), resulting in enhanced oxidative stress. In the colon, nitrosamines enter through systemic circulation.¹⁸ High levels of nitric oxide (NO) contribute to oxidative stress as well as promote the formation of reactive nitrogen species (RNS). RNS can react with superoxide (O_2^-) to produce peroxynitrite, a highly toxic compound. Peroxynitrite is capable of oxidizing lipids, proteins, and DNA, thereby increasing the risk of cellular and tissue damage.¹⁹

As depicted in Figure 3, there was a marked decrease in Lieberkuhn crypt height in the negative control (K-) and treatment (K+ and P) groups compared to the normal control (KN) group. Lieberkuhn crypts are intestinal glands that secrete ions and water, immunoglobulin A (IgA), and antimicrobial peptides into the intestinal lumen. These

secretions support the preservation of the epithelial surface and enhance the efficiency of nutrient absorption in the intestine. Each crypt contains several stem cells that are essential for repopulating the intestinal epithelial lining. When these stem cells are disrupted, the structure of the crypts becomes altered, leading to epithelial damage and

apoptosis.²⁰ Goblet cells, which are responsible for mucus production, also originate from these stem cells located at the base of the crypts. Therefore, stem cell impairment may disrupt goblet cell proliferation and contribute to a reduction in goblet cell numbers.²¹

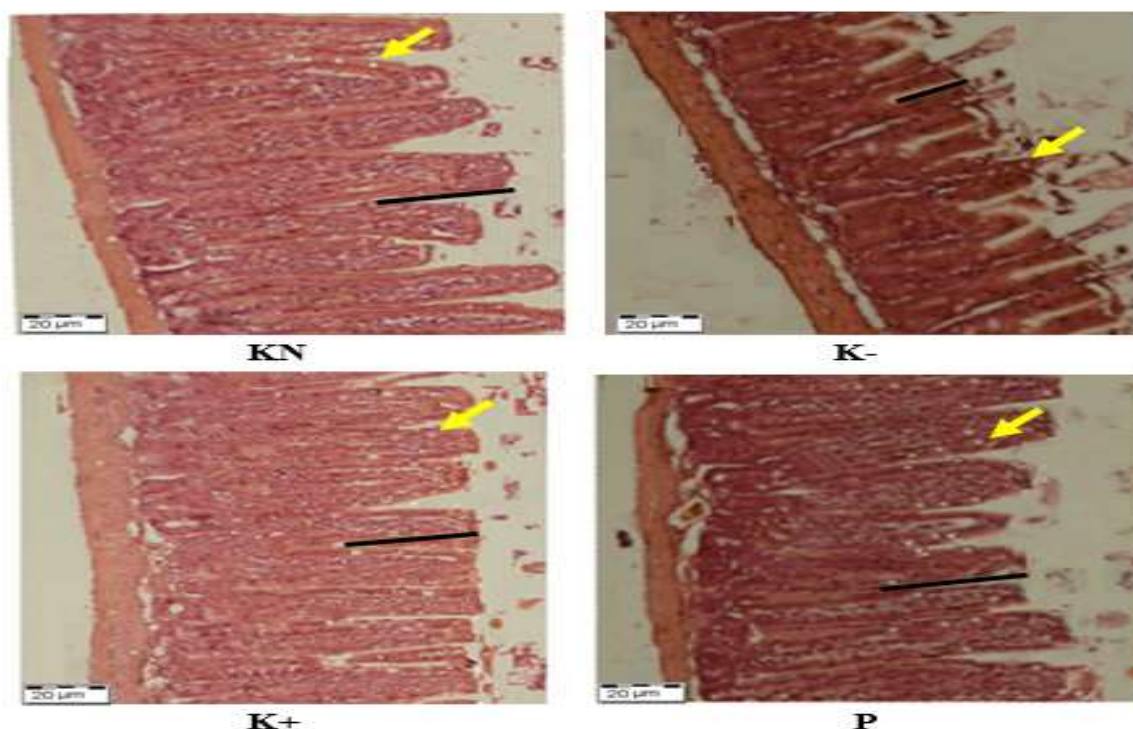


Figure 1: Photomicrograph of histological sections of mouse colon. **KN:** Normal control (given distilled water only); **K-:** Negative control (administered DEN at 100 mg/kg BW); **K+:** Positive control (administered DEN at 100 mg/kg BW + Doxorubicin at 10 mg/kg BW); **P:** (administered DEN at 100 mg/kg BW + *Ganoderma applanatum* extract at 150 mg/kg BW). Black line = height of Lieberkuhn crypt and yellow arrow = goblet cells. Magnification 100X.

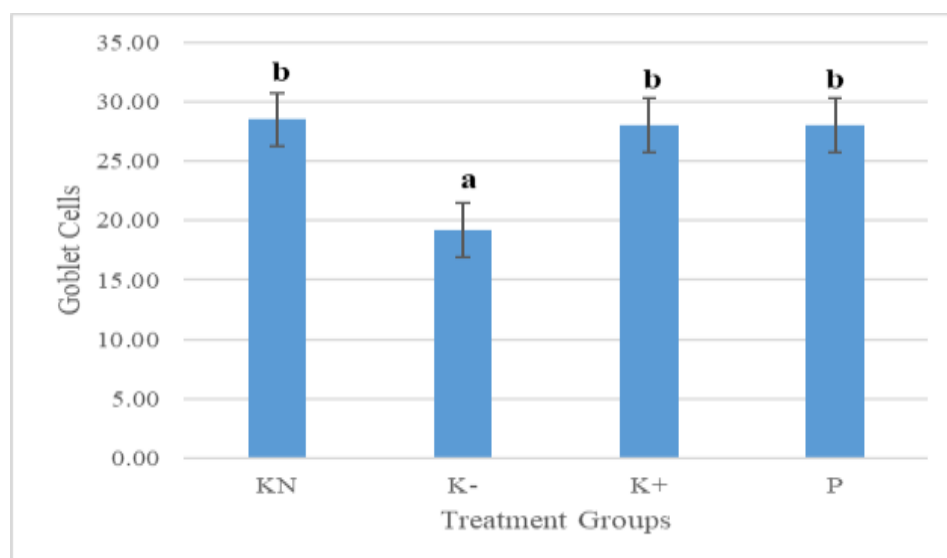


Figure 2: Number of colonic goblet cells following the administration of *Ganoderma applanatum* polysaccharide extract, DEN, and doxorubicin. Different letters indicate significant differences between treatments. **KN:** Normal control (given distilled water only); **K-:** Negative control (administered DEN at 100 mg/kg BW); **K+:** Positive control (administered DEN at 100 mg/kg BW + Doxorubicin at 10 mg/kg BW); **P:** (administered DEN at 100 mg/kg BW + *Ganoderma applanatum* extract at 150 mg/kg BW)

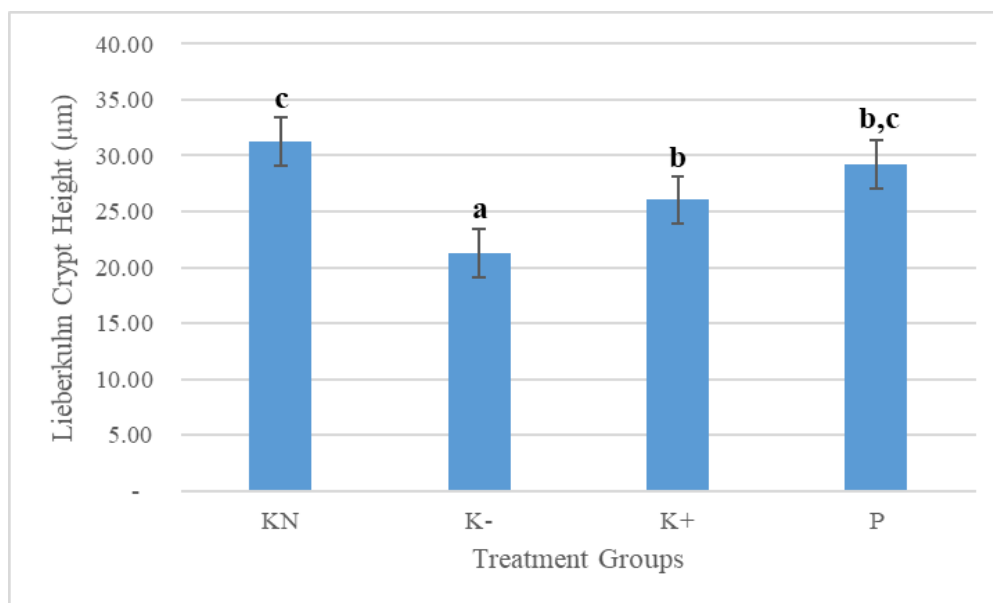


Figure 3: Lieberkuhn crypt height following the administration of *Ganoderma applanatum* polysaccharide extract, DEN, and doxorubicin. Different letters indicate significant differences between treatments. **KN:** Normal control (given distilled water only); **K-:** Negative control (administered DEN at 100 mg/kg BW); **K+:** Positive control (administered DEN at 100 mg/kg BW + Doxorubicin at 10 mg/kg BW); **P:** (administered DEN at 100 mg/kg BW + *Ganoderma applanatum* extract at 150 mg/kg BW).

The pro-apoptotic effects of natural plant extracts have been widely studied, including on cancer cells. A study that examined four African plant extracts on MCF-7 breast cancer cells showed that these extracts induced apoptosis through mitochondrial membrane depolarization and caspase activation. This mechanism is similar to the way DEN exposure triggers apoptosis in colon cells, leading to cell death and tissue disruption.²² These findings concur with the observed decrease in goblet cells due to apoptosis, suggesting a cell death pathway mediated by oxidative stress and activation of immune responses. DEN, acting as a free radical inducer, promotes oxidative stress and apoptosis, particularly affecting goblet cells on the colonic epithelium and stem cells in the Lieberkuhn crypts. Since goblet cells originate from bowel stem cells which reside at the bottom of the crypts, apoptosis-induced damage to these stem cells disrupts goblet cell proliferation.²⁷⁻²⁹ The administration of *G. applanatum* extract appears to prevent apoptosis, thereby maintaining goblet cell numbers and supporting mucosal protection.

On the other hand, Lieberkuhn crypt height was significantly elevated following the administration of *G. applanatum* extract compared to the negative control (K-) group. In addition, the crypt height in the *G. applanatum* extract (P) group was similar to those observed in the normal control (KN) group. These findings suggest that *G. applanatum* extract treatment was able to prevent the shortening of the crypts of Lieberkuhn. This effect is likely associated with the polysaccharide content present in the *G. applanatum* extract.

Effect of *G. applanatum* extract on CD4+ and CD8+ cells

Figure 4 presents the percentages of CD4+ and CD8+ cells across the experimental groups: KN (19.32% and 7.41%), K- (17.31% and 5.94%), K+ (21.84% and 8.03%), and P (21.98% and 8.34%) for CD4+ and CD8+ cells, respectively. As shown in Figure 5, the percentage of splenic CD4+ cells was lowest in the K- group, with percentage value of $17.31 \pm 2.80\%$, which was not significantly different from that of the normal control (KN) group ($19.32 \pm 3.11\%$), but was significantly lower compared to the positive control (K+), and extract-treated (P) groups, with percentage CD4+ cells of $21.84 \pm 1.85\%$, and $21.98 \pm 3.03\%$, respectively. Figure 6 shows the percentage of splenic CD8+ cells across the various groups. Again, the K- group showed the lowest value ($5.94 \pm 0.99\%$), which was not significant different compared to the KN group ($7.41 \pm 1.94\%$), but significantly lower than that of the K+ and P groups which had percentage CD8+ values of $8.03 \pm 1.17\%$, and $8.34 \pm 0.86\%$, respectively. In other words, the administration of *G.*

applanatum extract resulted in a significantly higher percentage of CD4+ and CD8+ cells compared to the negative control (K-) group.

These results suggest that intraperitoneal DEN injection may trigger a compensatory immune response, where other components of the immune system act to maintain immune cell production in the spleen. As a key immune organ, the spleen plays a crucial role in mounting immune responses, and its function can be compromised by immune dysregulation.²³

It is likely that DEN is recognized by alternative immune mechanisms, such as NK cells, which respond to tumor antigens by secreting cytotoxic proteins: perforin and granzyme that activate caspases to induce apoptosis. DEN exposure can enhance NK cell activation, potentially surpassing that in the control group. NK cell activity is also regulated by cytokines secreted by CD4+ cells. A possible explanation for the lack of significant CD8+ cell activation could be insufficient IL-2 cytokine production by CD4+ cells. Alternatively, DEN can be directly phagocytosed by macrophages, which leads to the release of proinflammatory cytokines, like TNF- α , IL-1, as well as IL-6. Although studies demonstrate that DEN increases TNF- α and IL-6 levels compared to normal conditions, this may not be sufficient to activate Th/CD4+ cells to produce lymphokines needed for an effective antitumor response.²⁴

The spleen, as the primary site for lymphocyte storage and adaptive immune initiation, also functions in blood filtration.²⁵ It produces antibodies and macrophages to combat foreign antigens. Splenic immune cells (splenocytes) are composed of various cell types such as T cells, B cells, macrophages, natural killer (NK) cells, and dendritic cells.²⁶

These data are consistent with prior studies indicating that *Ganoderma* extract can increase the proportion of CD4+ and CD8+ cells, as well as increase the overall leukocyte count in the murine splenocyte population. CD4+ and CD8+ cell activation is also influenced by cytokines produced through innate immune responses, particularly by macrophages (Kupffer cells), which help regulate the signalling pathways involved in CD4+ cell activation. Once activated, CD4+ cells release IL-2 and IFN- γ , cytokines that increase the expression of MHC class I and II expression and subsequently activate CD8+ cells.³⁰

In this study, administration of *G. applanatum* extract also significantly increased CD8+ cell levels. Other studies have shown that *Ganoderma* extract elevates levels of IL-2 and IFN- γ , which are crucial for the activation of CD8+ cells, macrophages, and cytolytic NK cells.³¹

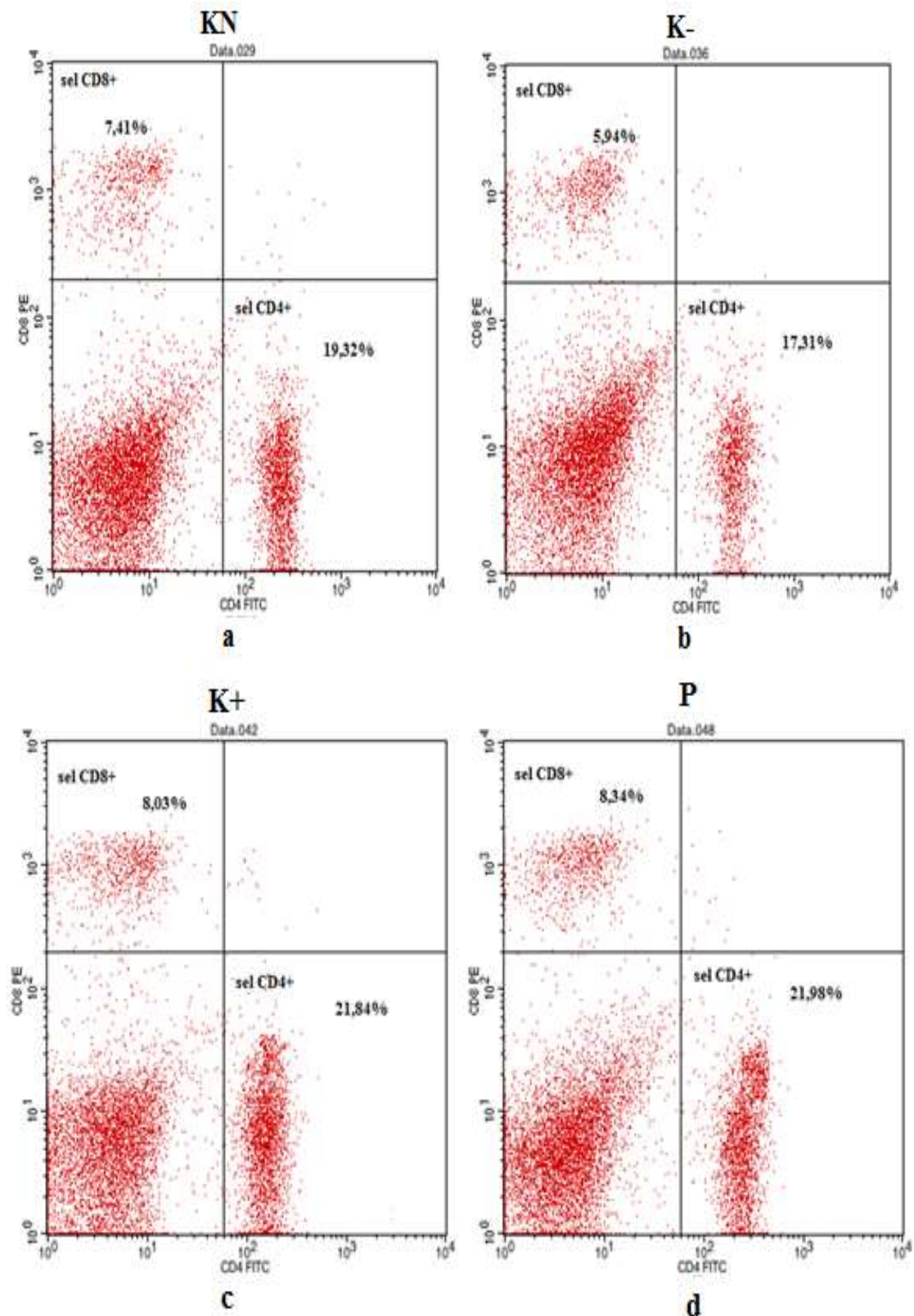


Figure 4: Percentage distribution of CD4+ and CD8+ cells in the spleen based on flow cytometry with BD Cell Quest software

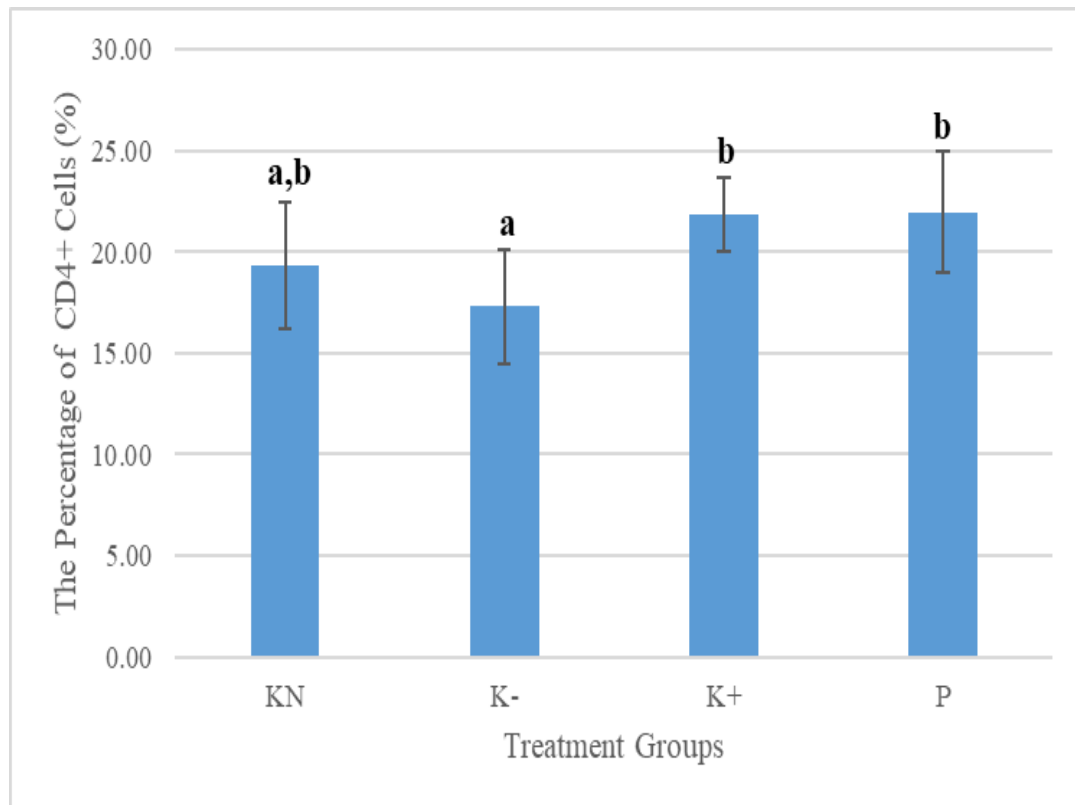


Figure 5: Percentage of CD4+ cells following the administration of *Ganoderma applanatum* polysaccharide extract, DEN, and doxorubicin. Different letters indicate significant differences between treatments. **KN:** Normal control (given distilled water only); **K-:** Negative control (administered DEN at 100 mg/kg BW); **K+:** Positive control (administered DEN at 100 mg/kg BW + Doxorubicin at 10 mg/kg BW); **P:** (administered DEN at 100 mg/kg BW + *Ganoderma applanatum* extract at 150 mg/kg BW).

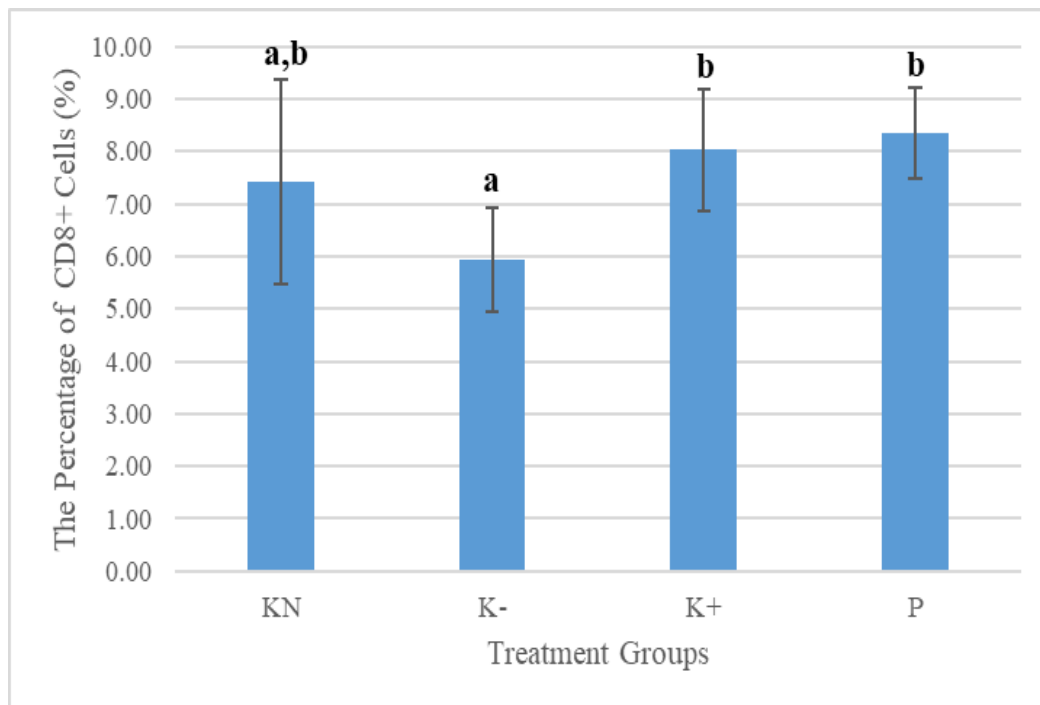


Figure 6: Percentage of CD4+ cells following the administration of *Ganoderma applanatum* polysaccharide extract, DEN, and doxorubicin. Different letters indicate significant differences between treatments. **KN:** Normal control (given distilled water only); **K-:** Negative control (administered DEN at 100 mg/kg BW); **K+:** Positive control (administered DEN at 100 mg/kg BW + Doxorubicin at 10 mg/kg BW); **P:** (administered DEN at 100 mg/kg BW + *Ganoderma applanatum* extract at 150 mg/kg BW).

Furthermore, CD4+ cells play an important role in antitumor immune responses by regulating CD8+ cell proliferation and differentiation.³² Treatment with *G. applanatum* extract at a dose of 150 mg/kg BW, administered after DEN induction, appeared to stimulate an enhanced immune response against tumour antigens. The innate immune response is first initiated by liver-resident macrophages (Kupffer cells), which phagocytose antigens and secrete cytokines to activate systemic immune defences.³³ These macrophages produce IL-1, IL-12, and TNF- α , which are noted to enhance NK cell cytotoxic activity.³⁴ The elevated cytokine levels subsequently reach the spleen, where they initiate an adaptive immune response by activating Th/CD4+ cells.³⁵ Enhanced antigen expression via MHC class II molecules, along with increased cytokine production by innate immune cells, plays a critical pathway in stimulating the adaptive immune response, primarily by activating Th/CD4+ cells. Once triggered, these cells differentiate into distinct subsets depending on the cytokines produced.^{36,37} Th1 cells release IL-2 and IFN- γ , drive the expansion of MHC class I and II molecules, increase CD8+ T cell activity, and stimulate natural killer (NK) cells and macrophages. On the other hand, Th2 cells unleash IL-4, IL-5, and IL-10, which facilitate the cultivation of B cells and their transformation into plasma cells capable of generating antibodies.³⁸ These antibodies bind to tumour antigens via their Fab regions, while their Fc regions bind to Fc receptors (FcR) on numerous immune-effector cells, including NK cells, macrophages, neutrophils, dendritic cells, eosinophils, basophils, and mast cells.³⁹ CD8+ cytotoxic T lymphocytes (CTLs) also contribute directly to antitumor immunity. These Tc/CD8+ cells are capable of recognizing tumour associated antigens as they appear on MHC class I molecules, which provokes their activation. These cells then release perforin and granzyme, cytotoxic proteins responsible for inducing cell death.⁴⁰ Perforin facilitates the entry of granzyme into target cells by forming pores in the tumour cell membrane. Once inside, granzyme activates

caspase-8, which in turn stimulates caspase-3.⁴¹ Caspase-3, an effector caspase, activates cytoplasmic DNase, resulting in DNA fragmentation and execution of the apoptotic program in target (cancer) cells.⁴² Additionally, activated CD8+ T cells are capable of expressing Fas ligand (FasL/CD95L), which is ligated to the Fas receptor (FasR/CD95R) on tumour cells, further promoting caspase activation and apoptosis.^{43,44}

Molecular docking results

Phytochemical investigation of *G. applanatum* identified 34 bioactive compounds with potential anticancer properties. From these, five compounds with the highest drug-likeness and solubility characteristics were selected. These include β -glucan, ganoderic acid-M, lucidenic acid-B, lucidenic acid-C, and mannitol. These compounds demonstrated promising potential for targeting CD4+ and CD8+ cells (Table 2). Molecular docking of the selected ligands with CD4+ and CD8+ receptors showed that all five compounds possess promising immunomodulatory activity by stimulating the formation of CD4+ and CD8+ cells. A more negative binding affinity value indicates a stronger interaction between the ligand and receptor. Lucidenic acid B exhibited the highest binding affinity for CD4+ simulation (-7.0 kcal/mol). Meanwhile, β -glucan showed the highest affinity for CD8+ (-7.1 kcal/mol). Most of the compounds demonstrated dominant polar hydrogen and van der Waals interactions rather than hydrophobic alkyl group interactions (Figure 7), which may contribute to their high solubility in plasma. This is further supported by molecular dynamics analysis, where the root mean square fluctuation (RMSF) values for the CD4-lucidenic acid B and CD8- β -glucan complexes were both <3 Å. An RMSF value below 3 Å indicates that the ligand-receptor complexes are relatively stable under physiological conditions (Figure 8).

Table 2: Molecular docking results of interaction between *Ganoderma applanatum* compounds and target receptors

Compound	Receptor	Binding affinity (kcal/mol)	Type of interaction	Amino acid residue
β -glucan	CD4+	-5.9	vdw	Ile34(A), Asn32(A), Ser31(A), Asp80(A), Ser79(A), Pro122(A), Asp78(A), Leu51(A)
			PHI	Arg54(A), Lys75(A), Lys50(A)
	CD8+	-7.1	vdw	Thr30(A), Gly32(A), Tyr51(A), Ser53(A), Asn55(A), Gln54(A), Pro29(A), Phe77(A), Gly74(A), Asp75(A), Leu26(A), Leu25(A)
			PHI	Val24(A), Arg72(A), Ser31(A)
Ganoderic acid-M	CD4+	-5.9	vdw	Asn30(A), Ser79(A), Tyr82(A), Ile36(A), Ser49(A), Asp78(A), Arg54(A), Asn32(A)
			HI	Pro122(A), Leu51(A), Lys50(A)
			PHI	Glu77(A), Asp80(A), Ser31(A)
	CD8+	-7.0	vdw	Phe107(A), Phe93(A), Pro46(A), Tyr103(A), Ile101(A)
			HI	His106(A)
			PHI	Ser1(A), Ser105(A), Gln38(A)
Lucidenic acid-B	CD4+	-7.0	vdw	Gln152(A), Trp157(A), Lys136(A), Leu149(A), Asn137(A), Val146(A), Ser145(A), Ile138(A), Gln148(A), Ser147(A)
			PHI	Glu150(A), Arg134(A), Ser132(A)

Lucidenic acid-C	CD8+	-7.0	vdw	Ala96(A), Leu97(A), Met102(A), Phe104(A), Leu36(A), Pro46(A), Phe48(A), Lys58(A)
			PHI	Ser31(A), Ser34(A), Ser95(A)
	CD4+	-6.7	vdw	Ser31(A), Ile34(A), Leu51(A), Glu77(A), Ile36(A), Asp78(A), Ser79(A)
			HI	Pro122(A), Lys50(A)
			PHI	Asp80(A), Tyr82(A), Asn30(A)
	CD8+	-6.9	vdw	Lys58(A), Phe48(A), Ser31(A), Leu97(A), Ser34(A), Ser95(A), Ala96(A)
Mannitol			HI	Pro46(A), Met102(A), Leu36(A), Phe104(A)
	CD4+	-4.7	vdw	Arg134(A), Pro133(A), Trp157(A), Val146(A), Ile138(A), Asn137(A), Arg131(A), Lys136(A), Leu149(A), Ser132(A), Gln152(A)
			PHI	Asp153(A), Glu150(A)
	CD8+	-4.3	vdw	Lys21(A), Leu20(A), Pro7(A), Val18(A)
			PHI	Glu19(A), Arg10(A), Trp12(A), Glu16(A), Thr17(A)

vdw: Van der Waals interaction; **HI:** Hydrophobic interaction; **PHI:** Polar Hydrogen interaction

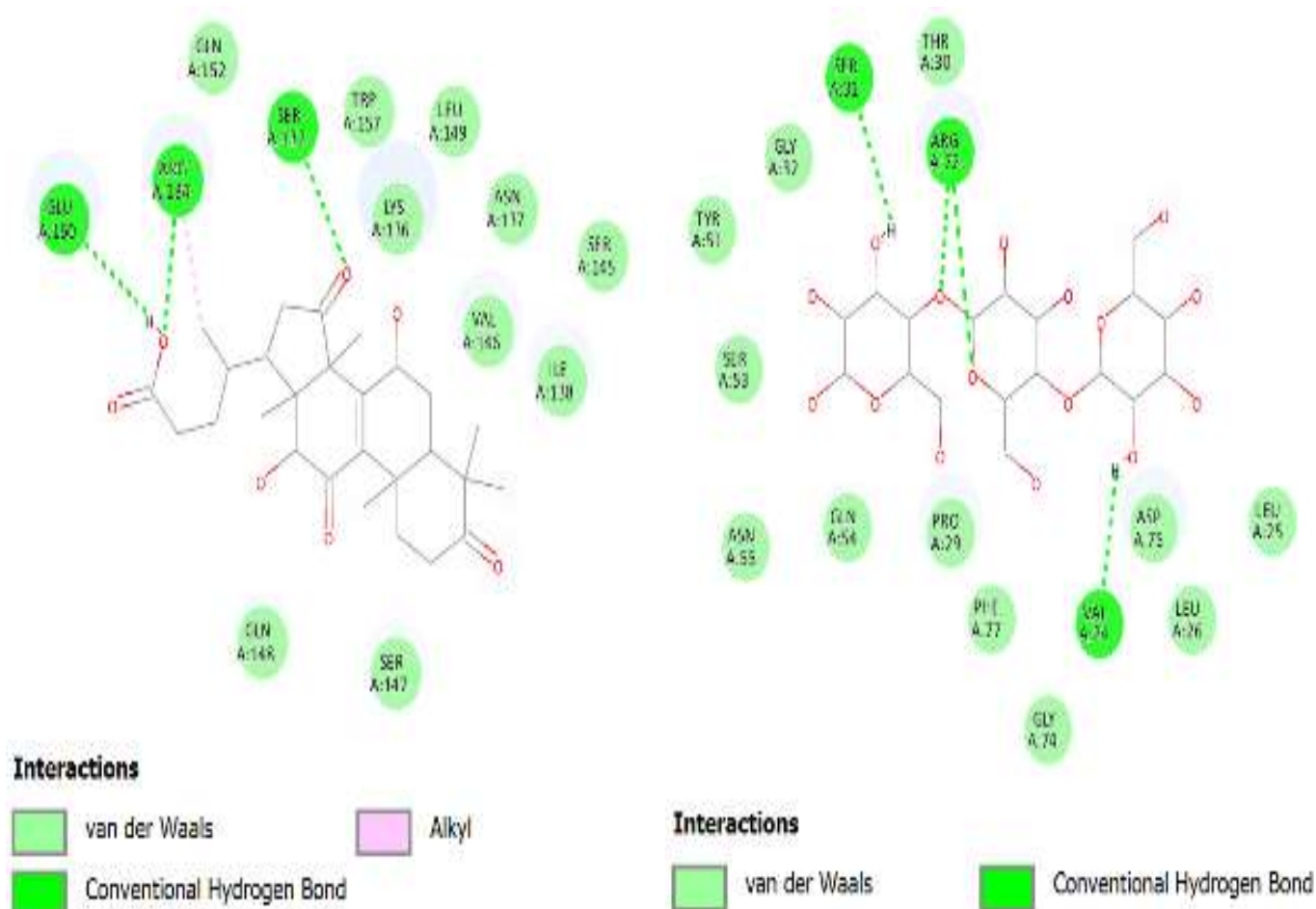


Figure 7: 2D visualization of ligand-protein complex. (A) Lucidenic acid and CD4+ cells; (B) β -glucan and CD8+ cells

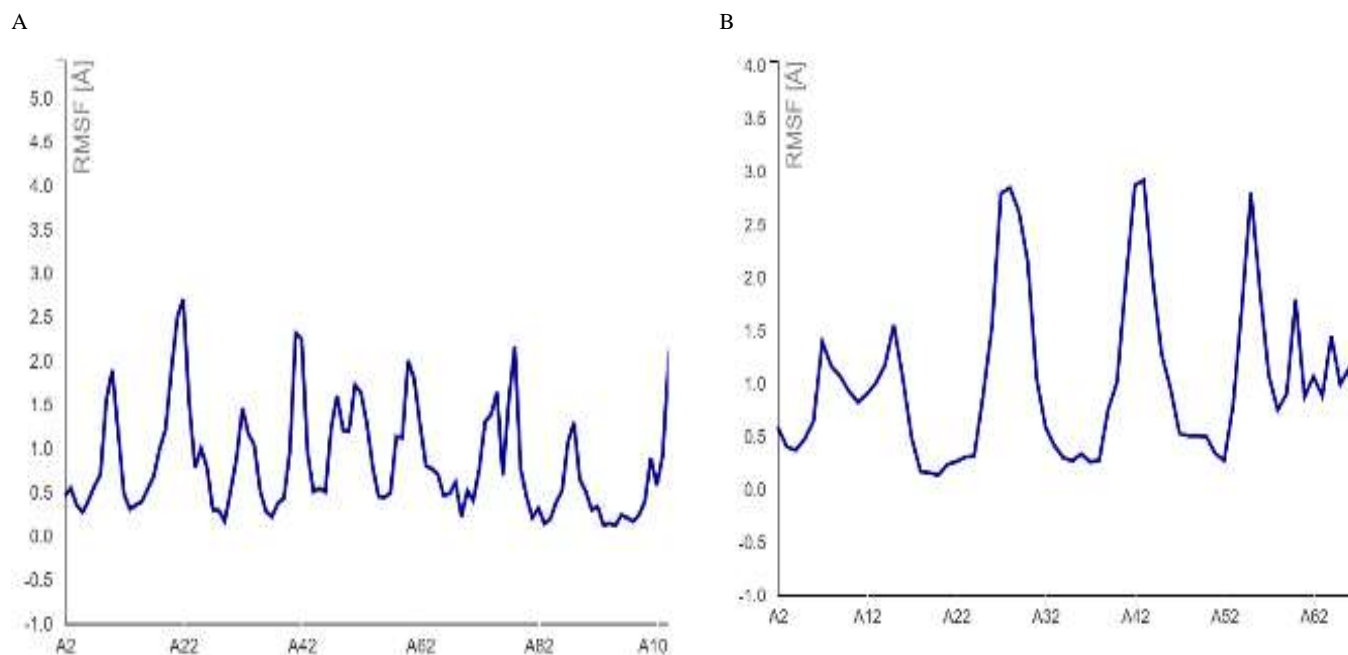


Figure 8: (A) Root mean square fluctuation of lucidenic acid-CD4+ cells complex, (B) Root mean square fluctuation of β -glucan-CD8+ cells complex.

Conclusion

The administration of *Ganoderma applanatum* extract (GAE) to mice induced with diethylnitrosamine (DEN) significantly improved colon histology by enhancing the amount of goblet cells and the height of Lieberkuhn's crypt. In particular, a significant enhancement in splenic CD4+ and CD8+ cell percentages was observed. Molecular docking analysis revealed that β -glucan exhibited the highest binding affinity for CD8+ cells, while lucidenic B had the strongest affinity for CD4+ cells. Furthermore, molecular dynamics simulations showed that the RMSFs of β -glucan-CD8+ and lucidenic acid-CD4+ complexes remained below 3 Å, indicating stable ligand-receptor interactions in the plasma. These findings suggest that *G. applanatum* has promising potential as an anti-colon cancer agent and immunomodulator. Future investigations will focus on clarifying the appropriate molecular mechanism, optimizing its therapeutic dose, and conducting preclinical and clinical studies to validate its safety and efficacy for potential medical applications.

Conflict of interest

The author's declare no conflicts of interest.

Authors' Declaration

The authors hereby declare that the work presented in this article is original and that any liability for claims relating to the content of this article will be borne by them.

Acknowledgements

This study was supported by Penelitian Unggulan Perguruan Tinggi (PUPT) Grant in 2016 from Universitas Airlangga, Indonesia.

References

- Dewi NNA, Pranata AANS, Suksmarini NMPW. KRAS Gene Mutations in Colorectal Cancer. *Andalas Med Med*. 2021; 44:117-125.
- Nikmah LM, Fajariyah S, Mahriani M. The Effect of Ethanol Extract *Curcuma longa* Rhizome (*Curcuma Longa*) to Histological Structure of Rat Rectum Induced Dextran Sodium Sulphate (DSS). *J Ilmu Dasar*. 2019; 20:13.
- Chaudhary D, Khatiwada S, Sah SK, Tamang MK, Bhattacharya S, Jha CB. Effect of Doxorubicin on Histomorphology of Liver of Wistar Albino Rats. *J Pharm Pharmacol*. 2016; 4:186-190.
- Mohebbati R, Abbsnezhad A, Khajavi Rad A, Mousavi SM, Haghshenas M. Effect of Hydroalcoholic Extract of *Nigella sativa* on Doxorubicin-Induced Functional Damage of Kidney in Rats. *Q Horiz Med Sci*. 2016; 22:13-20.
- Al Rabadi L and Bergan R. A Way Forward for Cancer Chemoprevention: Think Local. *Cancer Prev Res*. 2017; 10:14-35.
- Walker GM and White NA. Introduction to Fungal Physiology. In: *Fungi*. Wiley; 1-35p.
- Singdevsachan SK, Auroshree P, Mishra J, Baliyarsingh B, Tayung K, Thatoi H. Mushroom Polysaccharides as Potential Prebiotics with Their Antitumor and Immunomodulating Properties: A Review. *Bioact Carbohydr Diet Fibre*. 2016; 7:1-14.
- Chowdhury M, Kubra K, Ahmed S. Screening of Antimicrobial, Antioxidant Properties and Bioactive Compounds of Some Edible Mushrooms Cultivated in Bangladesh. *Ann Clin Microbiol Antimicrob*. 2015; 14:8.
- Chavez-Gonzalez ML, Balagurusamy N, Aguilar C. Advances in Food Bioproducts and Bioprocessing Technologies (1st ed.). Boca Raton, FL: CRC Press, Taylor & Francis Group; 2020; Contemporary Food Engineering: CRC Press. doi:10.1201/9780429331817.
- Hidayati S, Agustin AT, Sari EK, Sari SM, Destiawan RA, Silvana WA. Phytochemical Profiling and Antidiabetic Evaluation of *Peperomia pellucida* as a Potential Alpha Glucosidase Inhibitor. *Biodiversitas J Biol Divers*. 2023; 24(11):2023. doi:10.13057/biodiv/d241116.
- Alifiansyah MRT, Herdiansyah MA, Pratiwi RC, Pramesti RP, Hafsyah NW. QSAR of Acyl Alizarin Red Biocompound Derivatives of *Rubia tinctorum* Roots and Its ADMET Properties as Anti-Breast Cancer Candidates Against MMP-9 Protein Receptor: *In Silico* Study. *Food Syst*. 2024; 7:312-320.
- Herdiansyah MA, Rizaldy R, Alifiansyah MR, Fetty AJT, Anggraini D. Molecular Interaction Analysis of Ferulic Acid (4-hydroxy-3-methoxycinnamic Acid) as Main Bioactive Compound from Palm Oil Waste Against MCF-7 Receptors: An *In Silico* Study. *Narra J*. 2024; 4:e775.

13. Shivanika C, Deepak Kumar S, Ragunathan V, Tiwari P, Sumitha A, Brindha Devi P. Molecular Docking, Validation, Dynamics Simulations, and Pharmacokinetic Prediction of Natural Compounds Against the SARS-CoV-2 Main-Protease. *J Biomol Struct Dyn.* 2022; 40:585-611.
14. Bernal E, Serrano J, Perez A, Valero F, Antela A, Moreno S. The CD4:CD8 Ratio Is Associated with IMT Progression in HIV-Infected Patients on Antiretroviral Treatment. *J Int AIDS Soc.* 2014; 17(4 Suppl 3):19723. doi:10.7448/IAS.17.4.19723.
15. Birchenough GMH, Johansson ME, Gustafsson JK, Sepehri Z, Nyström EE, Arike L, Hansson GC. New Developments in Goblet Cell Mucus Secretion and Function. *Mucosal Immunol.* 2015; 8:712-719.
16. Paone P and Cani PD. Mucus Barrier, Mucins, and Gut Microbiota: The Expected Slimy Partners? *Gut.* 2020; 69:2232-2243. doi:10.1136/gutjnl-2020-322260.
17. Al-Kaseem M, Al-Assaf Z, Karabeet F. Determination of Seven Volatile N-Nitrosamines in Fast Food. *Pharmacol Pharm.* 2014; 5:195-203.
18. Adu AA, Sudiana K, Martini S, Widodo A, Widyanto RM. The Effect of Se'i (Smoked Beef) Toward the Improvement of the Bcl-2 Protein Expression on Colon Cells of Balb/c Strain Mice as a Carcinogenesis Indicator. *Indian J Public Health Res Dev.* 2018; 9:238.
19. Zhang F, Shi JJ, Thakur K, Zhang JG, Wei ZJ, Chen F. Anti-Cancerous Potential of Polysaccharide Fractions Extracted from Peony Seed Dreg on Various Human Cancer Cell Lines Via Cell Cycle Arrest and Apoptosis. *Front Pharmacol.* 2017; 8:102. doi:10.3389/fphar.2017.00102.
20. Galluzzi L, Vitale I, Aaronson SA, Abrams JM, Adam D, Agostinis P, Alnemri ES. Molecular Mechanisms of Cell Death: Recommendations of the Nomenclature Committee on Cell Death 2018. *Cell Death Differ.* 2018; 25:486-541.
21. He C, Gao H, Xin S, Zhang Y, Xue Q, Guan H, Zhang H. View from the Biological Property: Insight into the Functional Diversity and Complexity of the Gut Mucus. *Int J Mol Sci.* 2023; 24:4227.
22. Engel N, Falodun A, Kühn J, Ohlendorf B, Weisensee D, Efferth T. Pro-Apoptotic and Anti-Adhesive Effects of Four African Plant Extracts on The Breast Cancer Cell Line MCF-7. *BMC Complement Altern Med.* 2014; 14:1-13.
23. Lewis SM, Williams A, Eisenbarth SC. Structure and Function of the Immune System in the Spleen. *Sci Immunol.* 2019; 4(33):eaau6085. doi:10.1126/sciimmunol.aau6085.
24. Zhang Y, Li X, Li X. *Curcumae* Ameliorates Diethylnitrosamine-Induced Hepatocellular Carcinoma Via Alteration of Oxidative Stress, Inflammation and Gut Microbiota. *J Inflamm Res.* 2021; 14:5551-5566.
25. Murphy KM and Weaver C. No Title. 9th ed. Garland Science/Taylor & Francis Group, LLC; 2017.
26. Cho C-W, Han C, Rhee YK, Hwang JH, Choi MS, Hong HD. Cheonggukjang Polysaccharides Enhance Immune Activities and Prevent Cyclophosphamide-Induced Immunosuppression. *Int J Biol Macromol.* 2015; 72:519-525.
27. Bachelet I and Fuchs Y. Apoptotic Dysregulation Mediates Stem Cell Competition and Tissue Regeneration. *Nature Commun.* 2023; 14:1-20.
28. Delgado ME, Grabinger T, Brunner T. Cell Death at the Intestinal Epithelial Front Line. *FEBS J.* 2016; 283:2701-2719.
29. van Gorp C, De Lange IH, Massy KRI, Kessels L, Jobe AH, Cleutjens JPM, Kemp MW, Saito M, Usada H, Newnham J, Hütten M, Kramer BW, Zimmermann LJ, Wolfs TGAM. Intestinal Goblet Cell Loss During Chorioamnionitis in Fetal Lambs: Mechanistic Insights and Postnatal Implications. *Int J Mol Sci.* 2021; 22(4):1946. doi:10.3390/ijms22041946.
30. Kao CHJ, Jesuthasan AC, Bishop KS, Simmonds MSJ. Anti-Cancer Activities of *Ganoderma lucidum*: Active Ingredients and Pathways. *Funct Foods Heal Dis.* 2013; 3:48-65.
31. Cadar E, Negreanu-Pirjol T, Pascale C, Pascale C, Tudoran L, Iovanovici V, Trifan A. Natural Bio-Compounds from *Ganoderma lucidum* and Their Beneficial Biological Actions for Anticancer Application: A Review. *Antioxidants.* 2023; 12(11):1907. doi:<https://doi.org/10.3390/antiox12111907>.
32. Topchyan P and Lin S. The Role of CD4 T Cell Help in CD8 T Cell Differentiation and Function During Chronic Infection and Cancer. *Immune Netw.* 2023; 23:1-21.
33. Hirayama D and Lida T. The Phagocytic Function of Macrophage-Enforcing Innate Immunity and Tissue Homeostasis. *Int J Mol Sci.* 2017; 19(1):92. doi:10.3390/ijms19010092.
34. Duque GA and Descoteaux A. Macrophage Cytokines: Involvement in Immunity and Infectious Diseases. *Front Immunol.* 2014; 5:1-12.
35. Meager A and Wadhwa M. An Overview of Cytokine Regulation of Inflammation and Immunity. In: eLS. John Wiley & Sons, Ltd; 2013. doi:10.1002/9780470015902.a0024658.
36. Roche PA, and Furuta K. The ins and outs of MHC class II-mediated antigen processing and presentation. *Nat Rev Immunol.* 2015; 15(4):203-216.
37. Broeke T, Wubbolts R, Stoorvogel W. MHC Class II Antigen Presentation by Dendritic Cells Regulated Through Endosomal Sorting. *Cold Spring Harb Perspect Biol.* 2013; 5:1-21.
38. Sun L, Su Y, Jiao A, Wang X, Zhang B. T Cells in Health and Disease. *Sig Transduct Target Ther.* 2023; 8(1):235. doi:10.1038/s41392-023-01471-y.
39. van Erp EA, Luytjes W, Ferwerda G, van Kasteren PB. Fc-Mediated Antibody Effector Functions During Respiratory Syncytial Virus Infection and Disease. *Front Immunol.* 2019; 10:548. doi:10.3389/fimmu.2019.00548.
40. Koh C, Lee S, Kwak M, Yun H, Kim MS. CD8 T-Cell Subsets: Heterogeneity, Functions, and Therapeutic Potential. *Exp Mol Med.* 2023; 55:2287-2299.
41. Beaudouin J and Watzl C. Single-Fluorescent Protein Reporters Allow Parallel Quantification of Natural Killer Cell-Mediated Granzyme and Caspase Activities in Single Target Cells. *Front Immunol.* 2018; 9:1840. doi:10.3389/fimmu.2018.01840.
42. Noor Z, Ahmad H, Ain Q, Khan F, Ali A, Khan A. Clinics in Oncology Caspase 3 and Its Role in the Pathogenesis of Cancer. *Clin Oncol.* 2022; 7:1-10.
43. Peter M, Hadji A, Murmann A, Brockway S, Putzbach W, Pattanayak A, Ceppi P. The Role of CD95 and CD95 Ligand in Cancer. *Cell Death Differ.* 2015; 22:1-11.
44. Yamada A, Arakaki R, Saito M, Kudo Y, Ishimaru N. Dual Role of Fas / FasL-Mediated Signal in Peripheral Immune Tolerance. *Front Immunol.* 2017; 8:1-10.